Membrane Stretch Accelerates Activation and Slow Inactivation in *Shaker* Channels with S3–S4 Linker Deletions

Iustin V. Tabarean and Catherine E. Morris
Ottawa Health Research Institute, Ottawa, Ontario K1Y 4E9, Canada

ABSTRACT At low $P_{open}(V)$ *Shaker* exhibits pronounced stretch-activation. Possible explanations for *Shaker*'s sensitivity to tension include 1) *Shaker* channels are sufficiently distensible that stretch produces novel channel states and 2) *Shaker* channels expand in the plane of the membrane during voltage gating. For channels expressed in oocytes, we compared effects of patch stretch on *Shaker* and mutants that retain their voltage-gating ability but activate sluggishly because all or most of the S3–S4 linker has been deleted. Deletants had 10, 5, or 0 amino acid (aa) linkers, whereas wild-type is 31 aa . In deletants, though activation is exceptionally slow, slow inactivation is exceptionally quick; the resulting kinetic match was a bonus that allowed effects of stretch to be followed simultaneously in both processes. With the intact linker, an ~3 orders of magnitude mismatch in the two processes makes this impracticable. Standard stretch stimuli increased the rates and extent of activation by about the same degree in wild type and deletants, with effects especially pronounced near the foot of $G(V)$. In deletants (where slow inactivation is strongly coupled to activation) stretch also accelerated slow inactivation. Maximum conductances were unaffected by stretch in all variants. In ramp clamp dose experiments, near-lytic patch stretch acted, for all variants, like a ~10 mV hyperpolarizing shift. These results suggested that, whether basal rates were high (wild type) or low (deletants), stretch acted by facilitating voltage-dependent activation. Channel activity was therefore simulated with/without "tension," tension being simulated via rate changes at voltage-dependent closed-closed transitions that might involve in-plane expansion (explanation 2). Simulated ΔP_{open} arising from ~2 kT of "mechanical gating energy" mimicked experimental effects seen with comfortably sub-lytic stretch.

INTRODUCTION

Voltage-gated channels are susceptible to various physical factors including pressure (Conti et al., 1984; Meyer and Heinemann, 1997), temperature (Rodriguez et al., 1998), osmolarity (Zimmerberg et al., 1990), and membrane tension (Gu et al., 2001). In situ, susceptible channels may avoid tension through cellular mechanoprotection (Morris, 2001), possibly including channel-specific strategies. Our aim was to examine the inherent mechanosusceptibility of voltage gating, and so we expressed *Shaker* channels heterologously and used a preparation (oocyte patches, pipette suction) with a well-characterized ability to subject channels to bilayer tension (Zhang and Hamill, 2000).

Voltage-gated channels reveal no unified picture of mechanosusceptibility. In *Shaker* (Gu et al., 2001), reversible dose-dependent stretch-activation occurs at low prestretch $P_{open}(V)$. This occurs at tensions that affect most eukaryotic mechanosensitive channels and at lower tensions than needed for bacterial channels (Sachs and Morris, 1998; Hamill and Martinac, 2001). Stretch irreversibly alters the function of skeletal muscle Na channel α-subunits (Tabarean et al., 1999; Shcherbatko et al., 1999). Co-expressed with its auxiliary β-subunit, the α-subunit shows normal fast gating and no response to membrane tension, but without β, the α-subunit exhibits anomalous slow inactivation that, during stretch, speeds up until the normal rate (that with β) is attained (Tabarean et al., 1999). Recombinant N-type Ca^{2+} channels in whole-cell clamp show reversible increases in peak current (no shift in activation) with stretch (Calabrese et al., 2001), as do L-type Ca^{2+} currents of vascular smooth muscle (Langton, 1993; Holm et al., 2000). Whether any voltage-gated channels generate physiological or pathological mechanosignals is an open question.

Hyperbaric pressure effects on the gating of squid voltage-gated Na^+ and K^+ channels (Conti et al., 1982a,b, 1984) suggested that a late voltage-activation step involves a volume increase. This could be consistent with stretch-activation but would not explain effects reported for Ca^{2+} channels. In voltage-gated K^+, Na^+, and Ca^{2+} channels, the voltage sensor motif is conserved (Yellen, 1998), but beyond that there is enormous interchannel diversity. If voltage gating is fundamentally stretch-sensitive, this might be masked in fully fledged channels, so we are probing simplified channels from the "primitive" end of the spectrum.

Previously (Gu et al., 2001) in addition to steady-state stretch-activation at the foot of $G(V)$ in *Shaker* we observed, at high P_{open}, reversible stretch-inactivation. We thought this might arise from channel deformations whose specifics varied with varying channel microenvironments (Gu et al., 2001). In the present study, however, stretch-inactivation was never observed and we have been unable to determine why not. Curiously, stretch-inactivation of other channel types has also either been reported as sporadic compared to stretch-activation (Morris and Sigurdson, 1989) or has

Submitted October 3, 2001, and accepted for publication February 22, 2002.

Address reprint requests to Catherine E. Morris, Neuroscience, Ottawa Health Research Institute, Ottawa Hospital, 725 Parkdale Ave, Ottawa, Ontario K1Y 4E9, Canada. Tel.: 613-798-5555, ext. 18608; Fax: 613-761-5330; E-mail: cmorris@ohri.ca.

0006-3495/02/06/2982/13 $2.00

proved elusive (Franco and Lansman, 1990; Ji et al., 1998; Suzuki et al., 1999; Bourque and Chakfe, 2000). The simpler pattern of responses obtained here allow us to consider simpler working models.

Gonzalez et al. (2000) and Sorensen et al. (2000) showed that removing the extracellular linker between *Shaker* segments S3 and S4 dramatically slows and right-shifts but does not abolish voltage-dependent gating. The linker, thought to form a vestibule that augments the width of the electric field felt by S4, also increases the conformational flexibility or degrees of freedom of S4. Systematic deletion of linker residues indicated that during gating charge movements of activation, displacement of the rotating S4 perpendicular to the bilayer is minimal (Gonzalez et al., 2001). Our thinking in testing the effects of stretch on these mutants was that if membrane stretch literally deforms *Shaker* proteins, creating a novel voltage-gating reaction path (Gu et al., 2001), then mutants whose flexibility is diminished by loss of a coupling domain might be less deformable and therefore insusceptible to stretch. Alternately, with or without stretch, *Shaker* may follow an identical voltage-gating reaction path, with mechanical work summing with the usual electrical work to achieve activation. If mechanical and electrical work are interchangeable, then stretch-activation should be evident in any *Shaker* variant capable of voltage gating, regardless of its speed, degree of shift, etc. Effects of stretch on the deletants and *Shaker* were consistent with the idea that membrane stretch can substitute for depolarization.

MATERIALS AND METHODS

Channel expression in oocytes

Oocytes were defolliculated with collagenase (Sigma Type IA, 2 mg/ml in Ca-free OR2 medium). Stage V and VI oocytes were selected and injected with the cRNA (5–25 ng per oocyte) encoding *Shaker*H4Δ(6–46) with an added C-terminal 8-amino-acid epitope as previously, provided by C. Miller (Gu et al., 2001) (for our purposes, wild-type, w-t) or with S3–S4 deletants: *Shaker*H4Δ-Δ(330–360), 0aa mutant; *Shaker*H4Δ-Δ(330–355), 5aa mutant; or *Shaker*H4Δ-Δ(332–351), 10aa mutant (Gonzalez et al., 2000), kindly provided by Dr. R. Latorre. The oocytes were maintained at 18°C in OR2 solution supplemented with 100 μg/ml streptomycin and 100 IU/ml penicillin. The OR2 solution contained (in mM): 82.5 NaCl, 2.5 KCl, 1 $NaHPO_4$, 1 $CaCl_2$, 1 $MgCl_2$, 5 HEPES-acid, pH 7.4. Oocytes were used for experiments after 1–5 days.

Electrophysiological recording

For patch clamp, the vitelline was removed manually in a hyperosmolar solution. Cell-attached and inside-out configurations were used; 1 or 2 patches were made per oocyte. Pipettes (3–4.5 MΩ) were pulled from borosilicate (Garner, Claremont, CA, 1.15 mm inner diameter) using a L/M-3P-A puller (List Medical, Darmstadt, Germany). Because we studied stretch effects, our conditions differed somewhat from Gonzalez et al. (2000). They used only cell-attached macropatches (10–30 μm diameter) and a high K^+ pipette solution. Macropatches tolerate suction poorly, so we used patches of ~1.4 to 2 μm diameter. Currents (filtered at 5 kHz) were recorded using an Axopatch 200B (Axon Instruments, Foster City, CA) amplifier, and digitized using pClamp6 (Axon Instruments) software; A/D and D/A converters were Digidata 1200 (Axon Instruments). Currents were corrected for linear capacitative currents with the amplifier's compensation circuits and residual capacitative and leakage currents were corrected by linear subtraction.

The patch pipette solution contained (in mM): 140 NaCl, 5 KCl, 1 $MgCl_2$, and 5 HEPES, pH 7.4 with NaOH. In some voltage ramp experiments we replaced 75 mM NaCl with 75 mM KCl. The bath solution contained (in mM): 100 K-aspartate, 20 KCl, 1 $MgCl_2$, 1 EGTA, 5 HEPES-acid, pH adjusted to 7.4 with KOH. Experiments were performed at room temperature (21–23°C).

To inhibit endogenous cation channels, 20 μM gadolinium was included in the pipette, as noted. This right-shifted the I/V of the K^+ channels ~10–20 mV. The fragility of excised patches discouraged their routine use but we confirmed stretch effects in excised patches (not shown).

Measurement of pipette pressure

A pneumatic transducer tester (DPM-1B, Bio-Tek, Winooski, VT) was used to measure (in mm Hg) negative pressures applied via the patch pipette side port to stretch membrane patches. A manual valve was opened to bring the system to atmospheric pressure (0 mm Hg).

Data analysis

To quantitate the rising or decaying part of currents, traces were fitted with exponential functions using Clampfit (Axon Instruments). Results are presented, unless stated otherwise, as means ± S.D., and n represents the number of patches.

Kinetic simulations

To simulate $G(t)$ for multiple channels in a patch, we used the SIMU program in the QuB Suite (a software package for single channel analysis and kinetic simulations available as freeware from F. Sachs and A. Auerbach). To simulate step from a hyperpolarized holding potential to any test potential, the initial probability of state C1 was set to unity and all others to zero. Simulations include noise at the default level (5 kHz).

RESULTS

Channel characteristics

Fig. 1 shows current families for the control, *Shaker* w-t (wild-type or 31aa S3–S4 linker), and for the deletion mutants 10aa, 5aa, and 0aa recorded from patches without (left) and with (right) 20 μM gadolinium. As expected (Gonzalez et al., 2000) the mutants exhibited ultraslow right-shifted activation compared to *Shaker* w-t. Note the time scales used for mutants versus wild type.

A characteristic of the S3–S4 linker deletion mutants not emphasized earlier (Gonzalez et al., 2000) is their relatively rapid inactivation. Large sustained depolarizations yield the striking difference evident in Fig. 2, where normalized ~8 s traces for all variants are plotted together. All 3 mutants were half-inactivated by 2 s, which represents inactivation speeds ~5- to 10-fold faster than for wild type. The deletants' ultraslow activation plus unusually rapid inactivation proved useful because, for at least part of the voltage range, both processes could be resolved on a common time scale. For *Shaker* w-t, simultaneously resolving both was unwork-

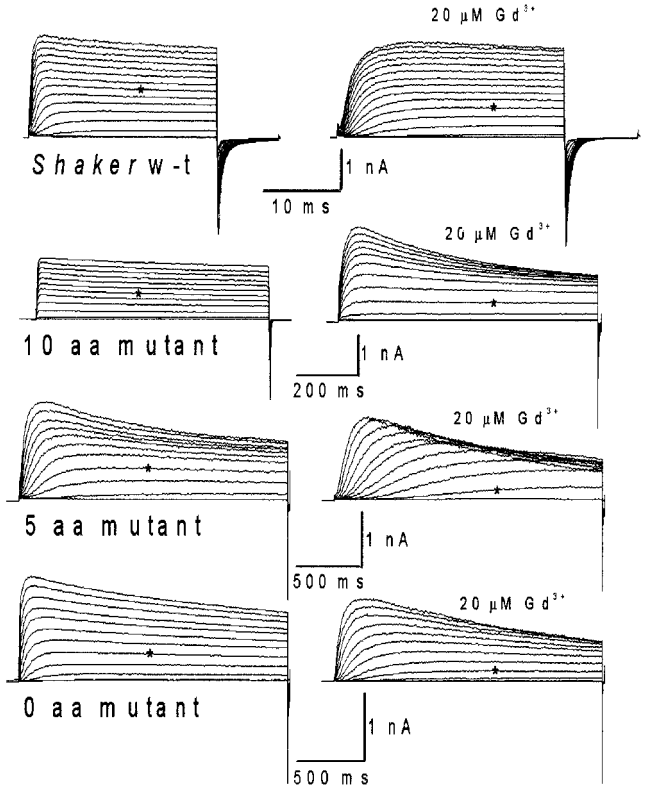

FIGURE 1 Channel characteristics. For *Shaker* w-t and three mutants, typical currents families are shown without and with Gd^{3+}. The time scale is radically shorter for w-t. Voltage steps from −90 mV were in 10 mV increments: w-t, −70 mV to 70 mV, w-t/Gd^{3+}, −40 mV to 100 mV; 10aa, −50 mV to 60 mV, 10aa/Gd^{3+}, −30 mV to 80 mV; 5aa, −30 mV to 70 mV, 5aa/Gd^{3+}, −10 mV to 90 mV; 0aa, −40 mV to 70 mV, 0aa/Gd^{3+}, −30 mV to 80 mV. Asterisks are placed over current elicited by stepping to 0 mV. Digitization rates: 10 kHz for w-t, 500 Hz for 10aa, 133 Hz for 5aa, and 0aa.

able because the time course mismatch exceeds 3 orders of magnitude (activation requires <10 ms, whereas slow inactivation requires >10,000 ms).

Effects of stretch on membrane leak and area

As illustrated in Fig. 3 *A*, stretching oocyte patches with gadolinium (−30 mm Hg, the standard throughout is illustrated here), did not detectably alter nonspecific leak or capacitance currents. This was true even with near-lytic stretch. Currents digitized at 100 kHz and elicited by 3-ms steps to −70 mV (which provides a good driving force for any nonspecific leak not blocked by gadolinium) without or with stretch overlapped completely. Capacitance increases due to membrane thinning during near-lytic stretch would be ~6% (Sachs, 1987), not resolvable by the voltage step method.

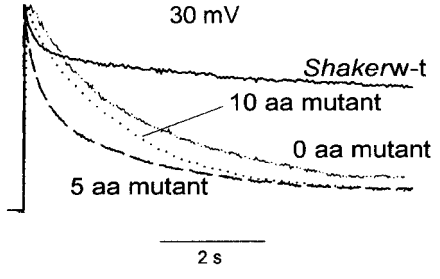

FIGURE 2 Slow inactivation in the four channel variants. Normalized current responses of the channel variants to long depolarizing steps from −90 mV to +30 mV, with 20 μM Gd^{3+}. Digitization, 83.3 Hz.

Though stretch did not detectably alter the quantity of patch membrane, it was still possible that stretch reversibly altered G_{max}. For example, *Shaker*-like channels target to lipid raft microdomains (Martens et al., 2000) whence they might be reversibly recruited during stretch. To examine G_{max} with stretch, I/V relations were generated by slow ramp clamps before, during, and after stretch. For these relatively slowly-inactivating channels, ramps (speeds adjusted for the channel variants) were better suited than step-families for monitoring G_{max} during stretch. At voltages above $V_{0.5}$ activation was not rate-limiting so G_{max} could be tested without/with stretch within seconds of each other (versus minutes for step-families). For *Shaker* w-t (Fig. 3 *B*, i) ($n = 12$), stretch reversibly increased ramp current over most of the voltage range but not at the large depolarizations associated with G_{max}. Current down-turn beyond 120 mV reflects slow inactivation. For 5aa ($n = 4$), slower time scale notwithstanding, stretch had the same effect as for *Shaker* w-t (Fig. 3 *B*, ii), a reversible hyperpolarizing shift. This was also observed for 0aa ($n = 4$) and 10aa ($n = 2$). Shifts did not arise as clamp artifacts, as can be seen in Fig. 3 *B*, iii, a ramp I/V for 0aa; here high-K^+ pipette solution was used so there were roughly equivalent driving forces for K^+ current at the foot and G_{max} regions (assuming $[K^+]_{in}$ was 120 mM, E_K was −7.3 mV). Stretch increased K^+ current at the foot of $G(V)$ without affecting G_{max}. These data indicate that effects of stretch on *Shaker* and its variants do not arise from changing channel numbers.

Effects of stretch on responses to step-depolarizations

For all variants, prolonged step-depolarizations near the foot of $G(V)$ elicited voltage-dependent currents that were dramatically and reversibly altered by stretch (Fig. 4). As with the ramp protocols, stimulus durations were adjusted for the variant-specific kinetics. In all four variants, peak current amplitude increased with stretch and for the mutants, inactivation also speeded up. A consequence of stretch-accelerated inactivation was that the stretch-current traces eventually crossed the before/after control traces (e.g., see 5aa). Note that, had we stepped back to the holding potential after, for example, 300 ms, rather than continuing for 3000 ms, only the stretch-activation of 5aa would have been observed. Alternately, had steady-state current been

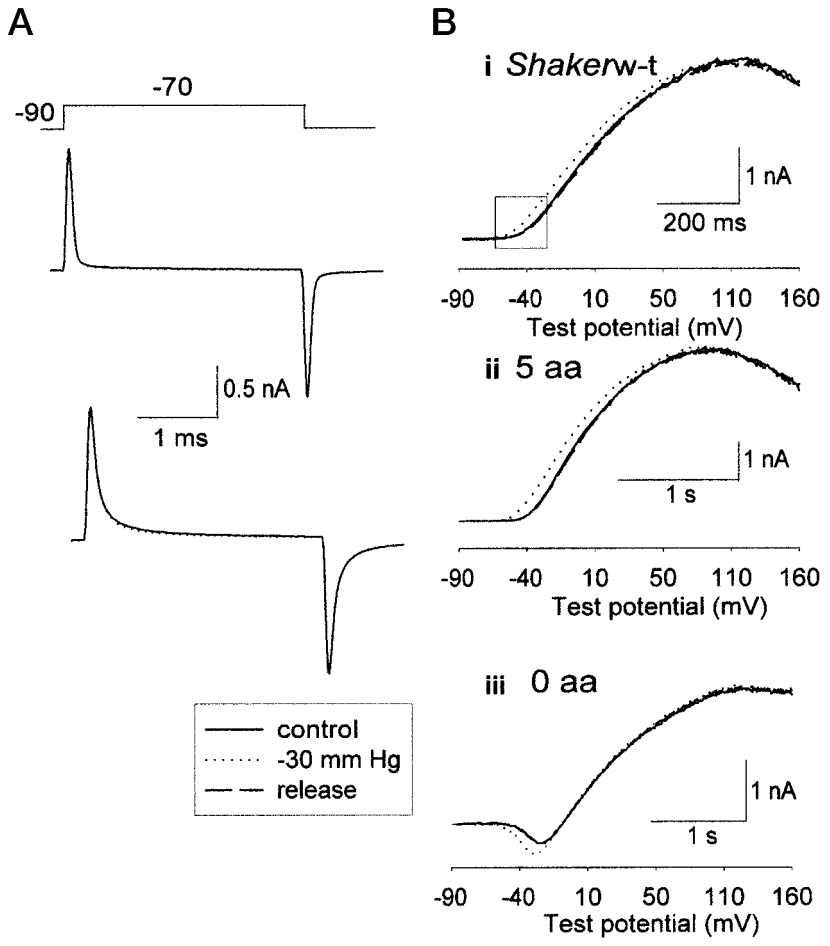

FIGURE 3 Testing for nonspecific effects of stretch. (*A*) Representative capacitative and leak currents, with 20 μM Gd^{3+}, elicited by 3 ms step depolarization from −90 mV to −70 mV in cell-attached patches from oocytes expressing *Shaker* w-t: control (*solid lines*) and during −30 mm Hg (*dotted lines*). Digitization, 10 kHz. (*B*) Representative currents elicited by depolarizing voltage ramps from −90 mV to +160 mV in cell-attached patches from oocytes expressing w-t (i), 5aa (ii) and 0aa (iii) channels. After returning to −90 mV and allowing a recovery (3–4 s), sustained suction (−30 mm Hg) was applied. Within 6–8 s (during suction) the ramp was repeated. Suction was released and 6–8 s later the ramp was repeated. Wherever figures indicate before, during, and after stretch (ramps or steps), this basic protocol applies. Throughout, traces during stretch are dotted lines, before and after are solid and interrupted lines, respectively. In iii, the pipette solution contained 80 mM KCl (instead of 5 mM) giving a reversal potential (E_{rev}) of approximately −5 mV, close to the estimated E_K of −7.3 mV. Digitization: 333 Hz (i and ii); 83 Hz (iii).

established and then a step-stretch applied, (during the period, for instance, between the arrows) the observed effect would have been designated "stretch-inactivation." As discussed later, however, we conclude that stretch effects on activation and inactivation occur via a single mechanism.

Figs. 5 and 6 illustrate, at higher time resolution, effects of a standard stretch stimulus at different voltages. Note that between-patch geometry differences mean that pressure *x* will not necessarily produce membrane tension *y*. Ideally, in any given patch, repeated pressure stimuli would produce an identical membrane tension but "patch history" studies (Hamill and McBride, 1997; Small and Morris, 1994) suggest that stretch stimuli can progressively diminish load bearing by the membrane skeleton, allowing bilayer load to increase. Since we went from hyperpolarized through to depolarized voltages, patch history bias would predicate smaller, not larger, bilayer tensions at the foot of $G(V)$. Stretch effects as depicted in Figs. 5 and 6 were observed consistently, that is, in 12 of 15 patches tested for w-t, 6 of 8 for 10aa, 14 of 18 for 5aa, and 10 of 13 for 0aa (patches from 4 batches of oocytes/channel variant; −30 mm Hg suction). Since stretch effects on *Shaker* channels are dose-dependent (see Gu et al., 2001 and below), it is reasonable that the standard stimulus was subliminal for some patches. Although −30 mm Hg will rupture macropatches, it can be characterized as producing "comfortably sub-lytic" membrane tensions in the present small-patch experiments (lytic tension in most biological membranes is ~10 mN/m; Morris and Homann, 2001). Fig. 5 illustrates data from *Shaker* w-t patches with gadolinium (*a*) and without (*b*). Gadolinium blocked endogenous mechanosensitive cation channels ($K_i < 10$ μM (Yang and Sachs, 1989)), ensuring they did

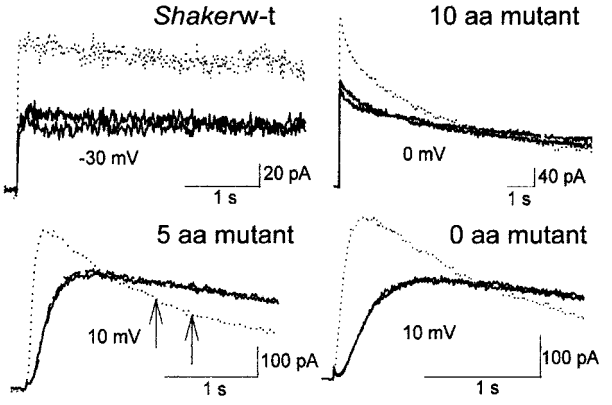

FIGURE 4 Reversible effects of stretch on the four channel variants. Currents from cell-attached patches during steps from −90 mV to the indicated voltage (near the foot of $G(V)$ for each channel type) for several seconds, as indicated. Before and after traces were typically as similar as repeat traces with no intervening stretch. 20 μM Gd^{3+} was used and −30 mm Hg.

not confound stretch responses. However, trivalent gadolinium has electrostatic effects on *Shaker* (Gu et al., 2001) and can alter bilayer mechanics (Ermakov et al., 2001). No-gadolinium controls were thus included to ascertain if stretch effects were secondary to gadolinium. Without or with gadolinium, stretch reversibly accelerated *Shaker* w-t

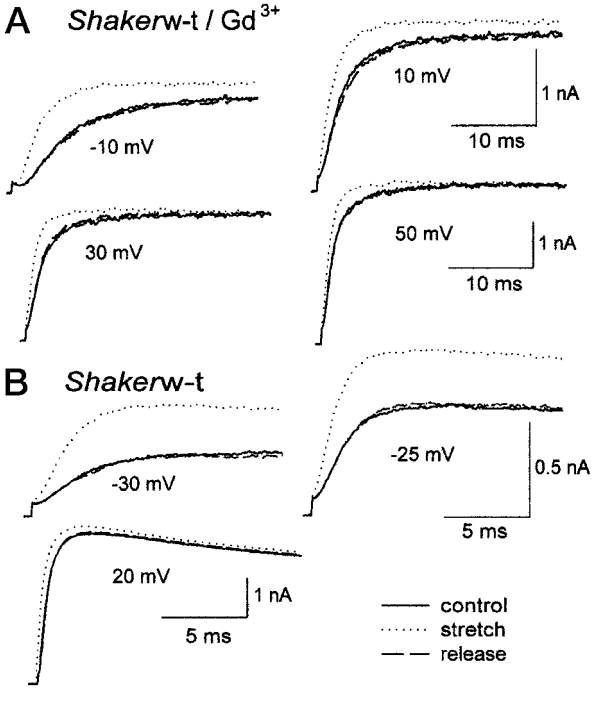

FIGURE 5 Effects of stretch on *Shaker* w-t at different voltages with 20 μM Gd^{3+} (*a*) and without (*b*). During steps (as indicated) from −90 mV, effects of stretch on steady-state levels and on the rise time were reversible and were especially pronounced nearer "the foot" of the $G(V)$; see −10 mV with Gd^{3+}, −30 mV without Gd^{3+}.

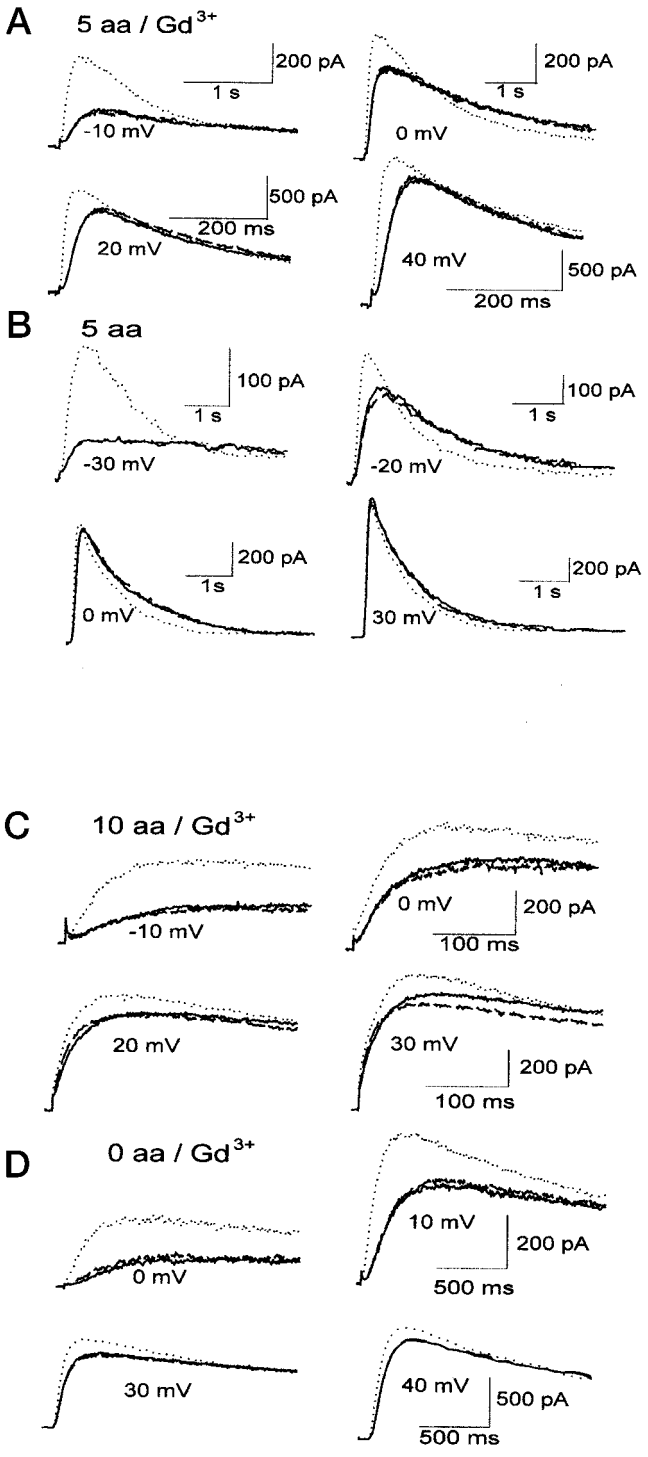

FIGURE 6 Effects of stretch on deletants at different voltages. (*a*) 5aa with 20 μM Gd^{3+}. (*b*) 5aa. (*c*) 10aa with 20 μM Gd^{3+}. (*d*) 0aa with 20 μM Gd^{3+}. Effects of stretch (peak current increase, faster activation and faster inactivation) were reversible and especially pronounced at more hyperpolarized potentials.

activation (i.e., the onset of current). Acceleration was most pronounced for V_m near the foot of $G(V)$ but was evident over the entire voltage range. Near the foot of $G(V)$ but not

at the top, stretch also increased steady-state *Shaker* w-t current. Stretch had no accelerating effect however, on slow inactivation, even when considerably longer depolarizations (~10 s) and larger stretch stimuli than shown here were used.

Fig. 6, *a* and *b*, presents similar data for 5aa, although the time scales are up to 100-fold longer than for *Shaker* w-t in Fig. 5. Again, both gadolinium and no-gadolinium traces are shown for a range of voltages. Near the foot of $G(V)$, stretch increased both the rate and extent of activation. Of the 4 variants, 5aa had the most rapid slow inactivation (Fig. 2), and stretch markedly accelerated this process, usually producing the "criss-crossing" effect noted earlier. Again, the overall impact of stretch on the currents was greatest at the more hyperpolarized voltages and this is seen, too, in the traces for 10aa and 0aa, as shown in Fig. 6, *c* and *d*. As with 5aa, stretch-accelerated inactivation was observed with 10aa and 0aa. Kinetic coupling between activation and slow inactivation (Loots and Isacoff, 1998) is evidently tighter in the deletants than in *Shaker* w-t and this may be echoed in the stretch responses.

For all variants (with and without gadolinium), Fig. 7 summarizes stretch/control ratios for activation rates and peak current amplitude at different voltages. Relative effects of stretch on both parameters were larger at more hyperpolarized voltages. There was, in other words, a clear trend for more pronounced effects of stretch near the foot of $G(V)$ in these voltage-gated channels.

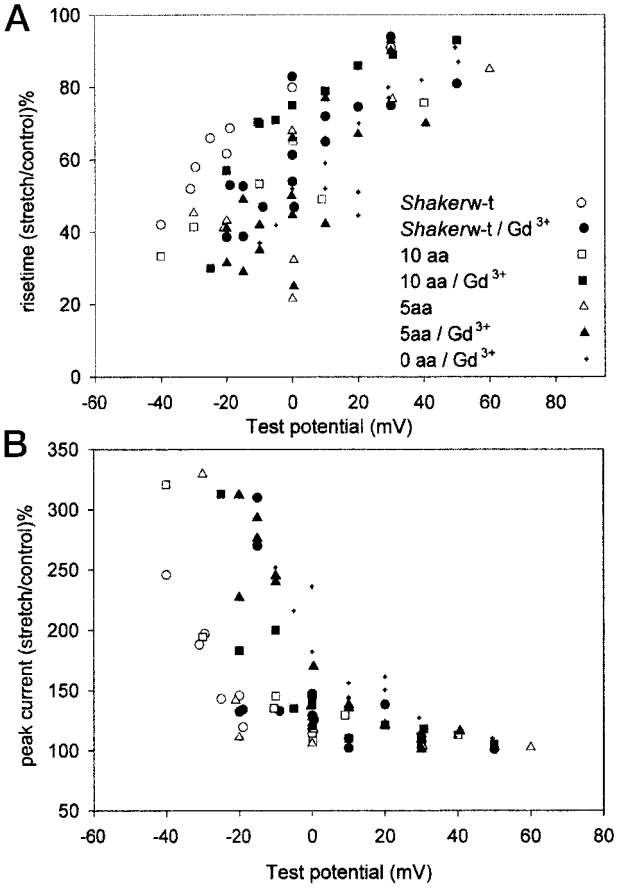

FIGURE 7 Effects of stretch were more pronounced at more hyperpolarized voltages. Pooled data from 9 patches for *Shaker* w-t, 5 for 10aa, 8 for 5aa, and 5 for 0aa. Patches which yielded data for at least two voltages are included in the plots. (*a*) Rise time constants without and with stretch were obtained by fitting an exponential to the rising phase of the current; plotted points representing the ratio (τ stretch)/(τ control). (*b*) The peak current amplitude was obtained without and with stretch; points represent the ratio (peak stretch)/(peak control). Where data points overlap, they have been slightly offset for display.

Stretch and deactivation and recovery from slow inactivation

We next tested the impact of stretch on deactivation from the open state. Tail currents (fit by a single exponential) were elicited by repolarization to −90 mV after activation at depolarized potentials (chosen appropriately for each variant). For all variants, deactivation time constants with stretch were within 20% of the control. Although mean τ-tail values with stretch were slightly smaller than control means (Table 1), this was not significant in paired *t*-tests (within-patch control versus stretch; $p > 0.05$). Note that if stretch caused a depolarizing voltage-clamp artifact (e.g., 5–10 mV), the result would be larger τ-tail values with stretch, since deactivation slows with depolarization in these channels, particularly in 10aa and 5aa (Fig. 5 in Gonzalez et al., 2000).

Stretch was tested on another process not tightly coupled to voltage gating, recovery from slow inactivation, using 5aa ($n = 4$) and 10aa ($n = 3$). The protocol used was: after a control pulse (−90 mV to +30 mV to −90 mV, 100 ms), channels were fully inactivated by stepping to 0 mV for 2 min. Next the membrane was repolarized to −90 mV and recovery monitored for ~40 s via test pulses (100-ms steps to +30 mV) at 0.9 Hz. The protocol was then repeated, except that immediately before ending the 2 min depolarization, stretch was applied. For each test pulse during recovery, a steady-state current ratio (test/control) was obtained and the time sequence was fitted with an exponential. Without and with stretch, the resulting recovery time constants were the same (paired *t*-tests, $p > 0.05$; means were

TABLE 1 Deactivation rate at −90 mV without and with stretch

Channel	*n*	Control τ-tail (ms)	Stretch* τ-tail (ms)	(τ stretch)/(τ control) × 100†
Wild type	10	1.1 ± 0.2	0.9 ± 0.1	90 ± 4.2% (0.84)
10aa	7	1.2 ± 0.3	1.2 ± 0.2	95 ± 4.1% (0.95)
5aa	12	1.9 ± 0.2	1.8 ± 0.2	94 ± 3.0% (0.94)
0aa	8	3.0 ± 0.5	2.7 ± 0.5	90 ± 4.0% (0.88)

*Produced by 25–30 mm Hg suction.
†From paired *t*-tests as indicated in the text; ratio from population means in brackets.

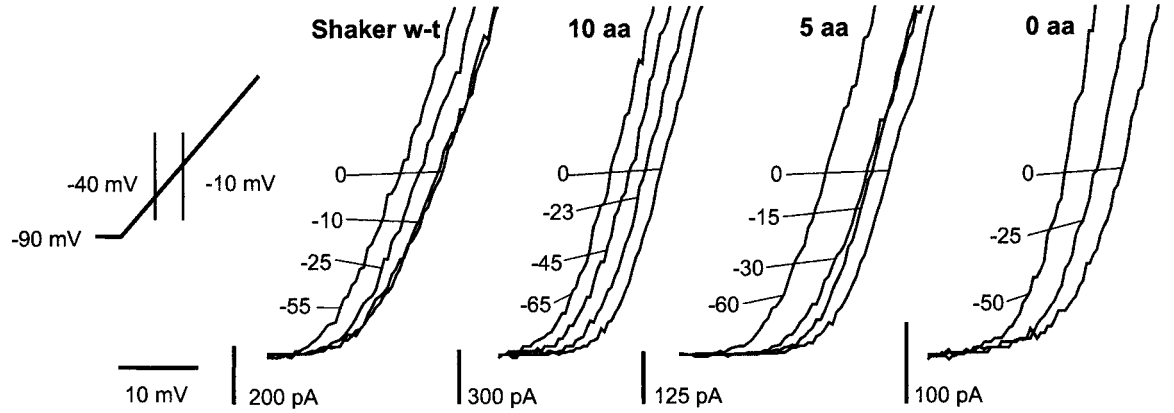

FIGURE 8 Membrane stretch shifts the I/V characteristics of the four channel variants toward negative potentials in a dose-dependent manner. The currents were elicited by depolarizing voltage ramps as described in Fig. 3. Here are presented excerpts from the ramp currents from the "foot" region of the I/Vs (the approximate voltage range excerpted is depicted at left). After recording 2–4 control ramps at 0 mm Hg (to check the stability of the recording) stretch was progressively increased to the indicated values (in mm Hg) between episodes (interval between ramps, 16 s). Gd^{3+} was used.

2.3 and 2.5 s (10aa) and 2.8 and 2.7 s (5aa), no-stretch and stretch, respectively).

Tension near the foot of *G*(*V*)

Thus, in its kinetic effects on *Shaker* and variants, stretch resembles depolarization but not, say, heat, since it does not speed all *Shaker's* processes. Only after its voltage sensors move to the "on" state (Yellen, 1998) does *Shaker* open. At the standard holding potential, −90 mV, the probability that sensors are on approaches zero and it required at least ~50 mV of depolarization to elicit currents. If stretch is a surrogate for depolarization, stretch must favor the on states. For a clearer picture of tension as gating energy, we explored the stretch effect noted in Fig. 3 *b*, namely the left-shifted I/V curves, over a dose response. As we do not image patches, we cannot rigorously estimate their tensions, but we took advantage of within-patch comparisons and increased tension along the continuum from none to lytic (biological membranes reach their elastic limits at ~10 mN/m; Morris and Homann, 2001). Two semi-quantitative questions about gating energy were asked. 1) As tension increases from rest to lytic, do slow ramp I/Vs (reflections of *G* (*V*)) shift progressively in a hyperpolarizing direction and, if so, how much hyperpolarization is equivalent to lytic tension? A variant on this is, can stretch added to a step depolarization elicit time-dependent currents when step depolarization itself is insufficient? 2) Do sluggish and fast channels show the same amount of hyperpolarizing shift at near-lytic tension (as expected if tension acts by favoring an expanded form of the channel and area changes in mutant and parent channels are similar) or do the sluggish deletion mutants require more mechanical gating energy than their fast parent (as expected if tension helps the gating mechanism overcome stiffness or internal friction)?

Fig. 8 illustrates dose-response voltage ramp traces near the foot of the ramp I/V curves (a box in Fig. 3 *b*, i shows the approximate regions excerpted in Fig. 8). Suction was progressively increased from zero in a series of increments until rupture occurred. Stretch produced hyperpolarizing I/V shifts for all variants. Maximal effects (i.e., shifts of the ramp I/V midpoint at the last ramp obtained before rupture, compared to that for the 0 mm Hg ramp) averaged ~10 mV for all variants (Table 2), and none differed significantly at the 0.05 level (*t*-tests) from any of the others.

If tension lowers energy barriers between voltage-dependent states, but engenders no novel channel conformations, then currents elicited "below" the normal foot of *G*(*V*) should be like those elicited with somewhat greater depolarization. Steps in the vicinity of the foot of *G*(*V*) were done to observe time-dependent currents associated with depolarization-plus-stretch at voltages that normally elicit no current. The threshold for voltage activation during steps from −90 mV was located (Table 3, column 2) then stretch was applied and activation was attempted during steps to voltages 10 mV or 15 mV hyperpolarized with respect to the patch's threshold. With all variants it was routinely possible to substitute for 10 mV of hyperpolarization with non-lytic stretch (see columns 3 and 4). As seen from the ramp experiments, however, this was close to the limit, since at steps 15 mV hyperpolarized wrt threshold (columns 5 and 6), even stretch due to −65 to −75 mm Hg (i.e., just below

TABLE 2 Maximal hyperpolarizing stretch-induced shifts of ramp I/V

Channel variant	Maximal shift at midpoint of I/V curve (mV ± S.D.)	*n*
w-t	8.8 ± 1.3	8
10aa	9.8 ± 3.2	7
5aa	10.1 ± 1.8	8
0aa	10.8 ± 2.3	8

TABLE 3 Activation at potentials more negative than the threshold

Channel variant	Threshold of voltage activation (mV)	Stretch applied (mm Hg)	Activation at 10 mV hyperpolarized wrt threshold	Stretch applied (mmHg)	Activation at 15 mV hyperpolarized wrt threshold
w-t	−30. . .−20	−40. . .−60	Yes (n=3of5)	up to −70	No (n=5)
10aa	−25. . .−15	−30. . .−60	Yes (n=3of4)	up to −70	No (n=5)
5aa	−10. . .0	−35. . .−55	Yes (n=4of5)	up to −75	No (n=3)
0aa	−15. . .−5	−40. . .−60	Yes (n=3of4)	up to −65	No (n=4)

the lytic limit for the patches) did not activate time-dependent currents. In these tests, as Fig. 9 illustrates for two of the variants, currents elicited by subthreshold voltages plus stretch were unremarkable-looking, as expected if stretch created no new "energy landscapes," but simply lowered barriers between existing states. In Fig. 9 *a*, *Shaker* w-t currents were detectably non-zero between −20 mV and −15 mV. Stretch (−30 mm Hg) had no detectable effect at −25 mV, but at −20 mV it yielded a current like that elicited by −15 mV without stretch (amplitude scales differ). As the well-resolved currents at −10 mV demonstrate, kinetics were not qualitatively altered by stretch. Fig. 9 *b* illustrates, for a 0aa patch, typical dose effects of tension around the foot of $G(V)$, with comfortably sub-lytic stretch

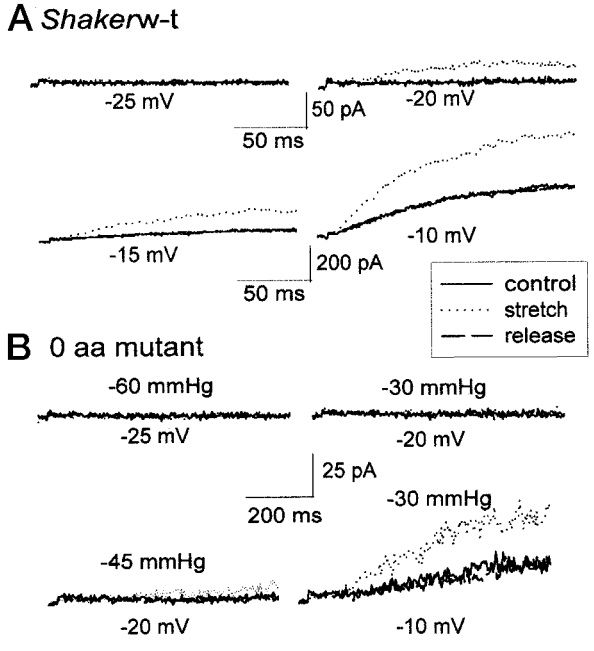

FIGURE 9 Activating current near the foot of $G(V)$. (*a*) *Shaker* w-t (before, during and after stretch) at voltages first within the foot region of $G(V)$, −25 mV, where no current was elicited with or without stretch (−30 mm Hg), and then in 5-mV increments. (*b*) 0aa currents before, during, and after stretch. At −25 mV stretch (up to −60 mm Hg) did not activate any current. At −20 mV, −45 mm Hg was required to activate current (−30 mm Hg did not activate current). At −10 mV, −30 mm Hg caused an increase (250%) in current amplitude and speeded activation (rise time was 37% of control). Gd^{3+} was used.

affecting currents like a small depolarization. Upon stepping to −25 mV, even −60 mm Hg could not elicit current. At −20 mV, −45 mm Hg yielded a small time-dependent current though −30 mm Hg did not enough. At −10 mV, however, it was evident that −30 mm Hg was adding gating energy to that provided by depolarization. Uncertainty about absolute membrane tensions notwithstanding, the stretch-dose tests from ramps and steps let us conclude the following: for *Shaker* type channels, near-lytic (∼10 mN/m) tension can substitute for the gating energy provided by 10 mV of depolarization and comfortably sub-lytic stretch (e.g., 1–5 mN/m) substitutes for ∼5 mV depolarization.

Stretch and inactivation in *Shaker* w-t

Previously on *Shaker* w-t, stretch applied at large depolarizations reversibly decreased steady-state currents (Gu et al., 2001). Because of the effect's speediness, we suggested it was stretch-deactivation; we termed it, however, "stretch-inactivation" (SI). SI was obtained repeatedly in both cell-attached and excised recordings and at both macroscopic and single channel levels. While not all patches showed SI, we attributed that to not looking exhaustively (i.e., at ever higher pressures until rupture). We sought without success to reproduce the phenomenon in this study. As measured by step families (Gu, 1999), or, as reported here, by ramps, stretch did not significantly decrease G_{max}. Given our new findings on the deletants, we thought SI might have been stretch-accelerated slow inactivation in *Shaker* w-t. We therefore looked exhaustively for this in *Shaker* w-t, using many patches from multiple oocyte batches, applying stretch at levels that were demonstrably near-lytic, applying maximally depolarizing stimuli, and using both cell-attached and excised patches. Never, however, did we observe stretch-acceleration of inactivation in *Shaker* w-t. This is illustrated for an excised patch in Fig. 10, which shows traces from a train of identical depolarizations (time for full recovery was provided depolarizations). Fig. 10 *a* follows the currents for ∼15 min following excision, before any stretch. Slow inactivation progressively speeded up following excision; evidently, unspecified features of intact membrane normally restrain the rate of slow inactivation. Once inactivation stabilized, stretch was applied (Fig. 10 *b*) but

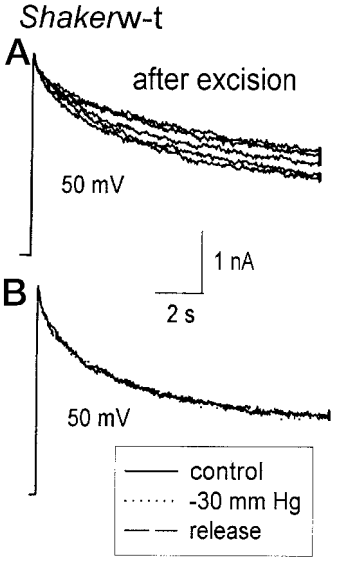

FIGURE 10 *Shaker* w-t currents from an excised patch elicited by steps from −90 mV to 50 mV. (*a*) During 15 min in the absence of stretch, the current decay became gradually faster. (*b*) In the same patch shortly thereafter, currents before, during and after stretch (−30 mm Hg).

had no effect on the rate of inactivation. Perhaps in our previous study, we somehow created situations in which stretch pulses transiently invoked the post-excision process of Fig. 10 *a*. We reiterate, however, that stretch procedures used here never accelerated slow inactivation in *Shaker* w-t, but only in the S3–S4 deletion mutants.

DISCUSSION

Mechanosusceptibility in voltage-gated *Shaker* type channels

The *Shaker* deletion mutants used show sluggish and right-shifted activation with reduced slope factors (Gonzalez et al., 2000; Sorensen et al., 2000) plus a property not previously noted, speedy slow inactivation. While linker excision constrains S4 mobility and hence the general internal flexibility of *Shaker*, deletants retain their fundamental voltage-dependence. We find that the inherent mechanosusceptibility of voltage-dependent gating, also, is essentially unchanged in the mutants.

Because the S3–S4 linker facilitates rotation (Gonzalez et al., 2001) of the principal part of the voltage-sensor, S4, we conclude (especially from 0aa) that *Shaker* mechanosusceptibility is unrelated to ease of motion here. Since the wild-type and mutants have dissimilar $G(V)$ midpoints and steepness factors, we also conclude that mechanosusceptibility is unrelated to electrostatic nuances determining these aspects of voltage gating, a point reinforced by the fact that trivalent gadolinium was not a factor. Since the stretch-induced hyperpolarizing shift was robust, we expect any *Shaker* variant capable of voltage gating would be similarly tension-sensitive. In other words, we postulate that mechanosusceptibility in *Shaker* type channels reflects a mechanical event inextricably tied to voltage gating. Channel expansion in the plane of the bilayer during voltage-dependent conformation changes could be responsible. Another class of explanation would be that bilayer deformation in the immediate vicinity of channel distorts the electric field. The two ideas need not be mutually exclusive. Segments S1-S3 seem to solvate in the bilayer (Monks et al., 1999; Hong and Miller, 2000) and if applied tension distorts/expands the bilayer-solvated periphery, this might favor stochastically expanded (activated?) states. However, even S5, where there appear to be large motions during gating (Elinder et al., 2001) may have several residues exposed to bilayer lipid (Hong and Miller, 2000), and possibly S4 (R. Guy, personal communication) too, so distortions at diverse channel sites could yield cross-talk between voltage and bilayer tension.

Stochastic channels with different sizes

Ionic and gating currents from squid axon K^+ and Na^+ channels at hyperbaric pressures led Conti, Stuhmer, and colleagues (Conti et al., 1982a,b; 1984) to suggest that the channels expand during voltage-dependent activation. Decreased rates of voltage-activation were observed with isotropic compression, whereas we observed increased rates with stretch; in barometric terms, stretch would be "decompression" confined to the bilayer plane. When Meyer and Heinemann (1997) applied the technique to recombinant *Shaker*, they too observed that pressure slowed activation (see their Fig. 5A). The data for Na^+ channel activation (Conti et al., 1982) yielded volume increase estimates of 26 $Å^3$ per gate (or ~5 $Å^3$ for a tetrameric channel). Our findings would be conceptually similar if "volume increase" involved expansion of bilayer-embedded channel protein. For slow inactivation, however, translating from tension to decompression (for most constructs, compression accelerated inactivation (Meyer and Heinemann, 1997)) predicts incorrectly that stretch would make slow inactivation slower.

Bilayer-embedded channels at stochastic equilibrium among large-area and small-area conformations are susceptible to tension (Guharay and Sachs, 1984; Sukharev et al., 2001; Sachs and Morris, 1998; Hamill and Martinac, 2001) because to go from smaller to larger the channel does work to displace (compress) adjacent bilayer. Increasing the membrane tension reduces the work needed. For transitions "larger→smaller" the opposite applies. In *Shaker*, depolarization causes S4s to relocate (Yellen, 1998) and this might involve a "Δarea" conformation change. *Shaker* dynamics inferred from combined gating/photochemical signals are agnostic on the question of expansion during voltage-activation; while the outermost dimensions in Bezanilla's (2000) cartoon channel, Fig. 16, are fixed (i.e., no expansion), the envelope of the S4s moves outward (i.e., expands)

to attain the "depolarized" conformation. Other evidence indicates that, perpendicular to the membrane, S4 excursions may be small (Gonzalez et al. 2001). Overall, the S4 dynamics evidence, the pressure and stretch effects on *Shaker*, and evidence from native voltage-gated channels in squid, make it hard to argue, a priori, for no-expansion models of voltage gating.

Simulating expanding *Shaker* type channels

The mechanosusceptibility we observed can be largely summarized as a reversible tension-dependent hyperpolarizing shift in $G(V)$. The time-dependent currents showed rate changes but otherwise, kinetic conservatism. To assess what kinetic changes might be associated with putative expansion during voltage-activation, we simulated channel activity using a simplified *Shaker* model of Aldrich and colleagues (e.g., Smith-Maxwell et al., 1998a, Fig. 4), modified only by addition of slow inactivation. For the deletants, the transition rates were reduced (Fig. 11). In keeping with our data, the behavior modeled was: 1) *Shaker* w-t: Stretch-induced increase in the rate and extent of activation, with this effect proportionally greater near the foot of $G(V)$. For the same stretch stimuli, no detectable effect on slow inactivation. 2) S3–S4 deletant mutants (especially 5aa): Comparable stretch-induced increase in the rate and extent of activation, with this effect proportionally greater near the foot of $G(V)$. For the same stretch stimuli, stretch-induced acceleration of slow inactivation.

Simulation runs at four voltages are shown in Fig. 11 for two kinetic schemes: *a* is a "5aa" model; *b* and *c* are for *Shaker* w-t. Because its kinetic fingerprint was more distinctive than *Shaker* w-t, 5aa was particularly helpful. Our thinking was that C1 = [all 4 subunits in rest position] and C5 = [all 4 subunits in active position] and that between C1↔C5 the channel expands (S4s, etc., repack). If there is zero cooperativity among subunits, then each C↔C transition has an identical Δarea increment whereas if there is maximal cooperativity, Δarea occurs exclusively at C4↔C5. Since evidence supports some cooperativity (Smith-Maxwell et al., 1998a,b), we weighted the Δarea toward C5; the precise assignments were arbitrary, but forward rates were multiplied and backward rates divided as shown (parentheses in "5aa"). Over a broad voltage range, small C3-C4 rate changes plus slightly larger C4-C5 rate changes (Fig. 11 *a*) mimicked 5aa behavior under comfortably sub-lytic stretch (Fig. 6, *a* and *b*, recalling that simulations are $G(t)$, whereas data are $I(t) = (V_m - E_K)G(t)$). The changes ($1.5 \times 1.5 \times 2 \times 2$) amount to a 9-fold increase in the forward reaction rate, or 2.2 kT of gating energy (from: $2.2 = \ln(9) = \Delta(P_{open}/P_{closed}) = \exp[\Delta\text{gating energy}]/kT$). These small "stretch" changes at the voltage-dependent steps C3↔C4↔C5 also dramatically augment a voltage-independent process (slow inactivation) near the foot of $G(V)$, as seen in the 5aa data. Both processes "react" because there is sufficiently tight kinetic coupling between the two. By contrast, when the wild type is modeled (Fig. 11, *b* and *c*), its disparate rates for activation and slow inactivation ensure that only activation responds during stretch simulations, also in keeping with our data.

Assuming our standard experimental −30 mm Hg yielded tensions of ~1 mN/m (= 1pN/nm = comfortably sub-lytic), we can estimate how much expansion in *Shaker* (Δarea) would be needed to account for the stretch responsiveness we observed. The rate changes in the 5aa stretch-simulation indicate that 1 pN/nm of membrane tension provides ~2.2 kT of gating energy. Given that kT = ~4 pN*nm, and that for an expanding two-state channel, mechanical gating energy = tension*Δarea, and that based on the kinetic simulation, (tension*Δarea)/kT = 2.2, the estimated in-plane Δarea going from deep closed to open would be $8.8 \sim = 9\ nm^2 = (30\ Å)^2$. If, however, the tension produced by −30 mm Hg was actually a near-lytic 5 mN/m, the estimated Δarea would be $1.8\ nm^2 = (13\ Å)^2$. To put the range ~2–9 nm^2 in context, note that mechano-gating of MscL (which requires ~20 kT of mechanical gating energy) involves an estimated Δarea of 19–22 nm^2 (Sukharev et al., 2001). For the *Shaker* context, the estimated expansion range (given in angstroms), $\sim(13\ Å)^2 - (30\ Å)^2$, is interesting to consider in light of data from Gonzalez et al. (2001) who suggest that their findings could mean that during activation, each S4 helix rotates away from S3 by ~3.2 Å. A cysteine mutagenesis approach (Elinder et al., 2001) suggests that near the channel's extracellular face there occur much larger movements of S4 with respect to S5 (>12 Å). How and if such movements would translate as in-plane Δarea depends on the details of repacking, but as a yardstick, note that on adding 3.2 Å to its radius, a 20 Å radius cylinder expands by $(21\ Å)^2$. *Shaker* is, in fact, a square tetramer (~ $(80\ Å)^2$) (Li et al., 1994) for which a 5% expansion (to $(82\ Å)^2$) would add $(18\ Å)^2$. Taken literally for a transmembrane protein, expansions of this order would generate a larger Δvolume, e.g., $\sim(20\ Å)^2 \times \sim 50\ Å = \sim(10\ Å)^3$, than the $\sim(5\ Å)^3$ suggested from the approach of Conti et al. (1982a; see above) and smaller volume than the $\sim(11\ Å)^3$ estimated (Zimmerberg et al., 1990) from the solute-accessible volume of squid K^+ channels. Overall, our results do not lead us to discard the idea that in-plane expansion during voltage-dependent activation could account for *Shaker* channel mechanosusceptibility. At this stage, kinetic studies (including gating currents) involving tensions of known value would be invaluable.

Gating energy from membrane voltage versus membrane tension

Together with the simulations, our data suggest that bilayer stretch acts as voltage surrogate for *Shaker*, but an important difference between mechanical and electrical gating energy should be highlighted. The "rest" position of voltage sensors requires stabilization by an intense electric field (~100 mV/5 nm) while the "active" position is favored by collapse

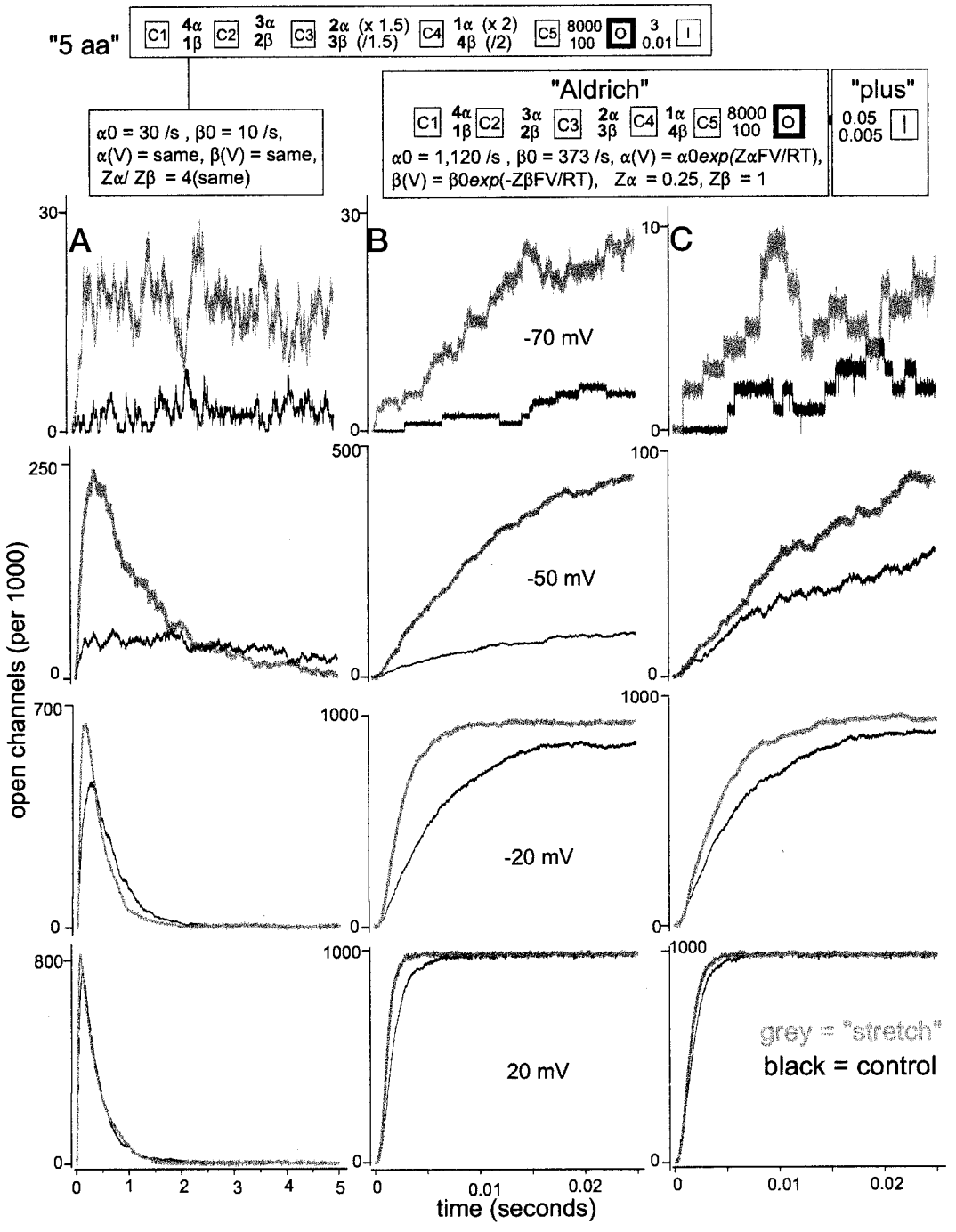

FIGURE 11 Simulations of channel activity in the 5aa mutant (*a*) and in *Shaker* w-t (*b*, *c*). Squares Cl-C5..O..I are closed, open, inactivated conformations, with forward (*top*) and backward (*bottom*) transition rates as indicated; voltage-dependent transitions are bolded. The exponential voltage-dependent rate constants are multiples of $\alpha 0$ and $\beta 0$ (values at 0 mV) and the equivalent charge, *z*, is as indicated in the "Aldrich" box. Slow inactivation is approximated by one state (but see Loots and Isacoff (1998) with 0.05 s^{-1} and 0.005 s^{-1} as forward and backward transition rates. For deletants, voltage-dependence was altered only in the frequency of transitions (small box below 5aa), with $\alpha 0$ and $\beta 0$ reduced from 1120 and 373 to 30 and 10 (i.e.,~40-fold). Voltage-independent rates at C5↔O were unchanged. Inactivation transitions at 3 s^{-1}, and 0.01 s^{-1} yielded 5aa-like inactivation. Gadolinium's assorted effects were not factored in. The noisy output "traces" of the simulator suite, QuB, reflect channel stochastics plus simulated background noise. With the driving force on *K* invariant, the simulated traces were essentially *G* (time), i.e., open channels per 1000 (each contributing a unit of conductance) at time, *t*, (column *a* and columns *b* and *c* have different time scales). When rate changes of 1.5×/and 2×/ at C3 C4 and C4 C5, respectively, were applied for 5aa (column *a*) and *Shaker* w-t (column *b*) models, this closely simulated experimental stretch effects. Simulations at voltages near the top of *G*(*V*) for *Shaker* w-t also mimicked experimental currents in that "stretch" speeded up activation but had no impact on slow inactivation. In column *c*, small rate increases are spread among *Shaker* w-t C2-C5 ($\alpha 0$ and $\beta 0$ change by factors of 1.05, 1.1, or 1.2), for an overall 1.9-fold (~2-fold) increase in the forward process. This serves to make the following point: our standard experimental stretch stimulus routinely produced substantially larger *I*(*t*) effects than seen here from a doubling of the overall forward activation rate.

of that field. By contrast, resting membrane tension represents an energetic minimum; both membrane expansion and compression require mechanical energy. Thus, for mechanical gating of *Shaker*, the channel-and-bilayer's mechanical potential must rise, whereas for voltage gating, electrical potential across channel-and-bilayer drops. If nature were attempting to optimize sensitivity, speed and reliability in a mechano-gating mechanism, surely it would not use the *Shaker* scenario. In this light, is it paradoxical that non-mechanotransducer *Shaker* is superior to MscL as a reporter of low bilayer tension? No, because the design features of MscL (Yoshimura et al., 2001) do not relate to a mere ability to increase P_{open} as a function of tension; MscL is designed to avoid any ΔP_{open} over an enormous range of tensions, and open only when lysis threatens. The biological interest of *Shaker*'s behavior is that it suggests that for multi-conformation membrane proteins, mechanosusceptibility may be a hard-to-avoid feature.

We thank Peter Juranka for preparing the RNA. This work was supported by a research grant to C.E.M. by NSERC, Canada.

REFERENCES

Bezanilla, F. 2000. The voltage sensor in voltage-dependent ion channels. *Physiol. Rev.* 80:555–592.

Bourque, C.W., and Y. Chakfe. 2000. Does a stretch-inactivated cation channel integrate osmotic and peptidergic signals? *Nat Neurosci.* 3:847–848.

Calabrese, B., P. F. Juranka, and C. E. Morris. 2001. Effects of membrane stretch on recombinant N-type calcium currents. *Biophys. J.* 80:119a.

Conti, F., R. Fioravanti, J. R. Segal, and W. Stuhmer. 1982a. Pressure dependence of the sodium currents of squid giant axon. *J. Membr. Biol.* 69:23–34.

Conti, F., R. Fioravanti, J. R. Segal, and W. Stuhmer. 1982b. Pressure dependence of the potassium currents of squid giant axon. *J. Membr. Biol.* 69:35–40.

Conti, F., I. Inoue, F. Kukita, and W. Stuhmer. 1984. Pressure dependence of sodium gating currents in the squid giant axon. *Eur. Biophys. J.* 11:137–147.

Elinder, F., R. Mannikko, and H. P. Larsson. 2001. S4 charges move close to residues in the pore domain during activation in a K channel. *J. Gen. Physiol.* 118:1–10.

Ermakov, Y. A., A. Z. Averbakh, A. I. Yusipovich, and S. Sukharev. 2001. Dipole potentials indicate restructuring of the membrane interface induced by gadolinium and beryllium ions. *Biophys. J.* 80:1851–1862.

Franco, A., Jr., and J. B. Lansman. 1990. Calcium entry through stretch-inactivated ion channels in mdx myotubes. *Nature.* 344:670–673.

Gonzalez, C., E. Rosenman, F. Bezanilla, O. Alvarez, and R. Latorre. 2000. Modulation of the Shaker K(+) channel gating kinetics by the S3–S4 linker. *J. Gen. Physiol.* 115:193–208.

Gonzalez, C., E. Rosenman, F. Bezanilla, O. Alvarez, and R. Latorre. 2001. Periodic perturbations in Shaker K^+ channel gating kinetics by deletions in the S3–S4 linker. *Proc. Natl. Acad. Sci. U.S.A.* 98:9617–9623.

Gu, C. X. 1999. Mechanosusceptibility of a voltage-dependent ion channel. Ph.D. thesis, University of Ottawa.

Gu, C. X., P. F. Juranka, and C. E. Morris. 2001. Stretch-activation and stretch-inactivation of Shaker-IR, a voltage-gated K channel. *Biophys. J.* 80:2678–2693.

Guharay, F., and F. Sachs. 1984. Stretch-activated single ion channel currents in tissue-cultured embryonic chick skeletal muscle. *J. Physiol.* 352:685–701.

Hamill, O. P., and B. Martinac. 2001. Molecular basis of mechanotransduction in living cells. *Physiol. Rev.* 81:685–740.

Hamill, O. P., and D. W. McBride, Jr. 1997. Induced membrane hypo/hyper-mechanosensitivity: a limitation of patch-clamp recording. *Annu. Rev. Physiol.* 59:621–631.

Holm, A. N., A., Rich., M. G. Sarr, and G. Farrugia. 2000. Whole cell current and membrane potential regulation by a human smooth muscle mechanosensitive calcium channel. *Am. J. Physiol.* 279:G1155–G1161.

Hong, K. H., and C. Miller. 2000. The lipid-protein interface of a Shaker K^+ channel. *J. Gen. Physiol.* 115:51–88.

Ji, S., S. A. John, Y. Lu, and J. N. Weiss. 1998. Mechanosensitivity of the cardiac muscarinic potassium channel: a novel property conferred by Kir3.4 subunit. *J. Biol. Chem.* 273:1324–1338.

Langton, P. D. 1993. Calcium channel currents recorded from isolated myocytes of rat basilar artery are stretch sensitive. *J. Physiol.* 471:1–11.

Li, M., N. Unwin, K. A. Stauffer, Y. N. Jan, and L. Y. Jan. 1994. Images of purified Shaker potassium channels. *Curr. Biol.* 4:110–115.

Loots, E., and E. Y. Isacoff. 1998. Protein rearrangements underlying slow inactivation of the Shaker K^+ channel. *J. Gen. Physiol.* 112:377–389.

Martens, J. R., R. Navarro-Polanco, E. A. Coppock, A. Nishiyama, L. Parshley, T. D. Grobaski, and M. M. Tamkun. 2000. Differential targeting of Shaker-like potassium channels to lipid rafts. *J. Biol. Chem.* 275:7443–7446.

Meyer, R., and S. H. Heinemann. 1997. Temperature and pressure dependence of Shaker K^+ channel N- and C-type inactivation. *Eur. Biophys. J.* 26:433–445.

Monks, S. A., D. J. Needleman, and C. Miller. 1999. Helical structure and packing orientation of the S2 segment in the Shaker K^+ channel. *J. Gen. Physiol.* 113:415–423.

Morris, C. E. 2001. Mechanoprotection of the plasma membrane in neurons and other non-erythroid cells by the spectrin-based membrane skeleton. *Cell. Mol. Biol. Lett.* 6:703–720.

Morris, C. E., and U. Homann. 2001. Cell surface area regulation and membrane tension. *J. Membr. Biol.* 179:79–102.

Morris, C. E., and W. J. Sigurdson. 1989. Stretch-inactivated ion channels coexist with stretch-activated ion channels. *Science.* 243:807–809.

Rodriguez, B. M., D. Sigg, and F. Bezanilla. 1998. Voltage gating of Shaker K^+ channels: the effect of temperature on ionic and gating currents. *J. Gen. Physiol.* 112:223–242.

Sachs, F. 1987. Baroreceptor mechanisms at the cellular level. *Fed. Proc.* 46:12–16.

Sachs, F., and C. E. Morris. 1998. Mechanosensitive ion channels in non-specialized cells. *Rev. Physiol. Biochem. Pharmacol.* 132:1–77.

Shcherbatko, A., F. Ono, G. Mandel, and P. Brehm. 1999. Voltage-dependent sodium channel function is regulated through membrane mechanics. *Biophys. J.* 77:1945–1959.

Small, D. L., and C. E. Morris. 1994. Delayed activation of single mechanosensitive channels in *Lymnaea* neurons. *Am. J. Physiol.* 267: C598–C606.

Smith-Maxwell, C. J., J. L. Ledwell, and R. W. Aldrich. 1998a. Role of the S4 in cooperativity of voltage-dependent potassium channel activation. *J. Gen. Physiol.* 111:399–420.

Smith-Maxwell, C. J., J. L. Ledwell, and R. W. Aldrich. 1998b. Uncharged S4 residues and cooperativity in voltage-dependent potassium channel activation *J. Gen. Physiol.* 111:421–439.

Sorensen, J. B., A. Cha, R. Latorre, E. Rosenman, and F. Bezanilla. 2000. Deletion of the S3–S4 linker in the Shaker potassium channel reveals two quenching groups near the outside of S4. *J. Gen. Physiol.* 115: 209–222.

Sukharev, S., S. R. Durell, and H. R. Guy. 2001. Structural models of the MscL gating mechanism. *Biophys. J.* 81:917–936.

Suzuki, M., J. Sato, K. Kutsuwada, G. Ooki, and M. Imai. 1999. Cloning of a stretch-inhibitable nonselective cation channel. *J. Biol. Chem.* 274:6330–6335.

Tabarean, IV, P. Juranka, and C. E. Morris. 1999. Membrane stretch affects gating modes of a skeletal muscle sodium channel. *Biophys. J.* 77:758–774.

Yang, X. C., and F. Sachs. 1989. Block of stretch-activated ion channels in *Xenopus* oocytes by gadolinium and calcium ions. *Science.* 243:1068–1071.

Yellen, G. 1998. The moving parts of voltage-gated ion channels. *Q. Rev. Biophys.* 31:239–295.

Yoshimura, K., A. Batiza, and C. Kung. 2001. Chemically charging the pore constriction opens the mechanosensitive channel mscl. *Biophys. J.* 80:2198–2206.

Zhang, Y., and O. P. Hamill. 2000. On the discrepancy between whole-cell and membrane patch mechanosensitivity in *Xenopus* oocytes. *J. Physiol.* 523:101–115.

Zimmerberg, J., F. Bezanilla, and V. A. Parsegian. 1990. Solute inaccessible aqueous volume changes during opening of the potassium channel of the squid giant axon. *Biophys. J.* 57:1049–1064.